Journal of Nuclear Materials 399 (2010) 189–199

Contents lists available at ScienceDirect

Journal of Nuclear Materials

journal homepage: www.elsevier.com/locate/jnucmat

U–Mo/Al–Si interaction: Influence of Si concentration

J. Allenou [a,b], H. Palancher [a,*], X. Iltis [a], M. Cornen [a,b], O. Tougait [b], R. Tucoulou [c], E. Welcomme [a], Ph. Martin [a], C. Valot [a], F. Charollais [a], M.C. Anselmet [a], P. Lemoine [d]

[a] CEA, DEN, DEC, F-13108, St. Paul Lez Durance Cedex, France
[b] Université de Rennes 1, UMR-CNRS 6226, Campus de Beaulieu, 35042 Rennes Cedex, France
[c] ESRF, 6 rue Jules Horowitz, 38042 Grenoble, France
[d] CEA, DEN, DSOE, 91191 Gif sur Yvette, France

ARTICLE INFO

Article history:
Received 25 June 2009
Accepted 27 January 2010

ABSTRACT

Within the framework of the development of low enriched nuclear fuels for research reactors, U–Mo/Al is the most promising option that has however to be optimised. Indeed at the U–Mo/Al interfaces between U–Mo particles and the Al matrix, an interaction layer grows under irradiation inducing an unacceptable fuel swelling.

Adding silicon in limited content into the Al matrix has clearly improved the in-pile fuel behaviour. This breakthrough is attributed to an U–Mo/Al–Si protective layer around U–Mo particles appeared during fuel manufacturing.

In this work, the evolution of the microstructure and composition of this protective layer with increasing Si concentrations in the Al matrix has been investigated. Conclusions are based on the characterization at the micrometer scale (X-ray diffraction and energy dispersive spectroscopy) of U–Mo7/Al–Si diffusion couples obtained by thermal annealing at 450 °C.

Two types of interaction layers have been evidenced depending on the Si content in the Al–Si alloy: the threshold value is found at about 5 wt.% but obviously evolves with temperature. It has been shown that for Si concentrations ranging from 2 to 10 wt.%, the U–Mo7/Al–Si interaction is bi-layered and the Si-rich part is located close to the Al–Si for low Si concentrations (below 5 wt.%) and close to the U–Mo for higher Si concentrations. For Si weight fraction in the Al alloy lower than 5 wt.%, the Si-rich sub-layer (close to Al–Si) consists of $U(Al, Si)_3 + UMo_2Al_{20}$, when the other sub-layer (close to U–Mo) is silicon free and made of UAl_3 and $U_6Mo_4Al_{43}$. For Si weight concentrations above 5 wt.%, the Si-rich part becomes $U_3(Si, Al)_5 + U(Al, Si)_3$ (close to U–Mo) and the other sub-layer (close to Al–Si) consists of $U(Al, Si)_3 + UMo_2Al_{20}$.

On the basis of these results and of a literature survey, a scheme is proposed to explain the formation of different types of ILs between U–Mo and Al–Si alloys (i.e. different protective layers).

1. Introduction

U–Mo/Al dispersed fuel is developed as a high-uranium-density fuel for research reactor (materials testing reactors, neutron sources, etc.) cores. Fuel elements generally consist of U–Mo meat (either U–Mo particles dispersed in an Al matrix or U–Mo foils) pressed between two Al sheets.

In operating conditions, a reaction between U–Mo particles or foils and the Al matrix occurs and can lead to an unacceptable irradiation behaviour [1]. Among numerous other propositions, the addition of Si into the Al matrix seems to be the most promising solution for tackling this issue.

On U–Mo/Al–Si fuel plates, a first interaction layer (IL) can grow in certain conditions before irradiation, i.e. during regular fabrication and especially during hot rolling and/or blister tests. In these cases, the so-formed IL seems to act as a protective coating. Indeed microstructural examinations carried out on ILs formed between U–Mo and Al–Si have shown that the decrease of the interaction rate seems to be linked to a silicon accumulation process in the IL (see for example [2–7] for out-of-pile and [8–10] for in-pile tests).

Nowadays, one of the most important remaining questions concerns the optimization of the silicon fraction to be added in the Al alloy: a compromise has to be found between a high enough Si concentration in the Al alloy leading to a sufficiently thick protective layer around each fissile particle and its necessary reduction for limiting back-end difficulties linked to the reprocessing of a fuel containing large Si fractions.

* Corresponding author. Tel.: +33 4 42 25 75 55; fax: +33 4 42 25 32 85.
E-mail address: herve.palancher@cea.fr (H. Palancher).

0022-3115/$ - see front matter © 2010 Elsevier B.V. All rights reserved.
doi:10.1016/j.jnucmat.2010.01.018

To reach that technological goal, a dedicated fundamental study of the U–Mo/Al–Si interaction is required.

Our previous work, performed on U–Mo/Al–Si diffusion couples (Si weight fraction ranging from 2 to 10 wt.%), has been focused on the evolution of the interaction layer (IL) thickness while Si content in the Al–Si alloy is increasing [5,6]. Two kinds of behaviour have to be considered with a threshold value of 5 wt.% of Si in the Al–Si alloy: below this value, the IL thickness decreases with increasing Si weight fraction, but above this value, a further increase in Si weight fraction has no influence on the IL thickness. This work has to be completed by a study of the microstructural characteristics and crystallographic compositions of the U–Mo/Al–Si interactions. This is the main goal of the present paper.

On a set of U–Mo/Al–Si diffusions couples (Si content ranging from 2 to 10 wt.%), characterizations were performed in two steps:

- First, the ILs are studied by SEM + EDS, in order to determine the layers and sub-layers thicknesses and elementary compositions.
- Then, X-ray diffraction experiments using micro-focused X-ray beams (μ-XRD) were performed on selected areas of the ILs.

The results of this work will be compared to existing data reported in literature and in particular to those dealing with synchrotron XRD measurements on U–Mo/Al–Si diffusion couples annealed at various temperatures [2–4].

Based on the conclusions of this comparison, a general scheme for the U–Mo/Al–Si interaction protective process will be proposed.

2. Experimental details

2.1. Raw materials

2.1.1. U–Mo alloys

Homogenized arc melted ingots of γ-U–Mo, containing 7 wt.% Mo (U–Mo7), were supplied by AREVA-CERCA (*a subsidiary of AREVA NP*) fuel manufacturer. Some uranium carbides (UC phase) are precipitated in the γ matrix.

2.1.2. Al alloys

Four aluminium alloys, with a Si content ranging from 2 to 10 wt.% (see Table 1) were supplied by ALCAN (France), in the form of rolled plates (thickness ~3 mm). At reception state, Si precipitates can be either inter- or intra-granular, depending on the alloys. After a heat treatment of 2 h at 450 °C (corresponding to that used for preparing diffusion couples), the Al grain size increases up to a few hundreds of micrometers. The Si precipitates also become larger and are only intergranular (Fig. 1).

2.2. Diffusion couples preparation

Diffusion couples were prepared with samples of $2 \times 5 \times 5$ mm^3, cut out from U–Mo ingots and Al alloys plates. Both parts were mechanically polished (to a final mirror polished state) and chemically etched. During the annealing, they were maintained in contact thanks to a clamping device. Two sets of four couples (one per Al–Si alloy) were prepared:

Table 1
Al alloys composition.

Al alloy	Al98–Si2 (Al–Si2)	4043 (Al–Si5)	4343 (Al–Si7)	4045 (Al–Si10)
Si (wt.%)	2	5	7.4	10
Other (wt.%)			0.21 Fe	
Al	Balance			

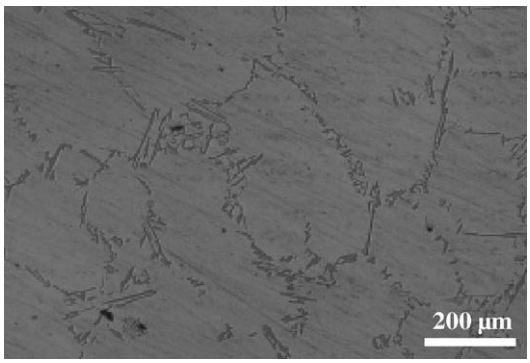

Fig. 1. Al–Si5 microstructure after annealing (450 °C–2 h) – optical microscopy.

- the first set was annealed at 450 °C for two hours, under Ar + 5% H_2 atmosphere, in order to induce the U–Mo/Al–Si interaction process,
- the second set underwent the same heat treatment followed by a complementary annealing of 2 months at 350 °C (performed in vacuum sealed fused quartz tubes).

The first annealing conditions were chosen to obtain thick ILs, with well defined stratifications (at least, in certain cases) and to develop as complete as possible interaction systems, in terms of concentration gradients and phases involved in the process (including eventual particularities linked to a progressive Si depletion process in the Al–Si alloy, in front of the interaction zone).

The second long annealing at a lower temperature was performed in order to obtain a better equilibrium state and study potential modifications in the IL characteristics without any significant increase in thickness of this area.

2.3. Characterizations

After their annealing, the diffusion couples were polished in cross-section. Each couple was characterized by SEM + EDS (Philips XL30 FEG SEM + EDAX EDS system), for determining the IL thickness, its possible stratification (presence of sub-layers) and its local elementary composition. The characterized areas were then marked with Vickers micro-indentations, to locate them precisely for further μ-XRD characterization.

The μ-XRD measurements were performed in reflection mode, on the ID22 beam line at the ESRF (European Synchrotron Radiation Facility) in Grenoble (France). To fulfil safety requirements, samples were conditioned under 70 μm thick kapton tape. The photon energy was set to 17 keV and the beam size on the samples was about 20×2 μm^2. The length of the beam print was positioned parallel to the reaction front and the sample was moved by micrometer step, perpendicularly to this front, between each acquisition. Diffraction data were collected and analyzed in the same way as that detailed previously [11].

3. Results

3.1. SEM/EDS characterization of ILs

As previously shown by Cornen et al. [5,6], the IL thicknesses, obtained at 450 °C, decrease when the Si content in Al increases, with a threshold value of about 5 wt.%. Beyond 5%, any increase in the Si content in the Al–Si alloy does not lead to a significant decrease of the IL thickness.

The SEM/EDS characterizations performed in this work have demonstrated that this critical value of 5 wt.% is also linked to significant changes in the IL microstructure and composition.

For this reason, three cases are taken into account in this work:

- the first deals with ILs obtained with a silicon weight fraction lower than 5 wt.% i.e. on the U–Mo7/Al–Si2 sample; this interaction type is labelled type 1 in the following,
- the second is typical of the ILs grown in diffusion couples with a high Si fraction (higher than 5 wt.%); these ILs are labelled type 2 and their characteristics have been defined thanks to the study of two samples (U–Mo7/Al–Si7 and U–Mo7/Al–Si10),
- the last concerns the ILs obtained in the U–Mo7/Al–Si5 sample.

The elementary compositions, determined by EDS, are given in at.%. Note that these values are semi-quantitative, their accuracy being estimated to about 1 at.%. As a consequence, low concentrations (for instance Mo concentrations) must be considered with care.

3.1.1. U–Mo/Al–Si interaction with Si < 5 wt.% (type 1)

Fig. 2 shows the microstructure and the compositions of an U–Mo7/Al–Si2 diffusion couple. This IL is three-layered. The (Al + Si)/(U + Mo) ratio (about 4.3) and the Mo and U concentrations (respectively 2 and 17 at.%) remain constant throughout the whole layer thickness. Thus, the elementary compositions of these sub-layers just differ in terms of Al and Si contents.

Close to the U–Mo side, the SEM micrograph shows that periodic layers have grown as reported in the U–Mo7/Al ILs [12]. This observation is in agreement with EDS results: Si is absent in this first area. In the intermediate area, the thickest (about 75% of the IL thickness), Si slightly increases up to 3 at.% in certain places (with no clear concentration gradient) and periodic layers are not present anymore. Finally the last sub-layer (located close to the Al–Si side), is enriched in Si (about 13 at.%).

3.1.2. U–Mo/Al–Si interaction with Si > 5 wt.% (type 2)

Fig. 3 is related to ILs grown in the U–Mo7/Al–Si7 (Fig. 3a) and U–Mo7/Al–Si10 (Fig. 3b) systems. It shows that this type of IL is also three-layered, the second sub-layer being thin (about 10% of the IL thickness) and perhaps corresponding only to a transition area.

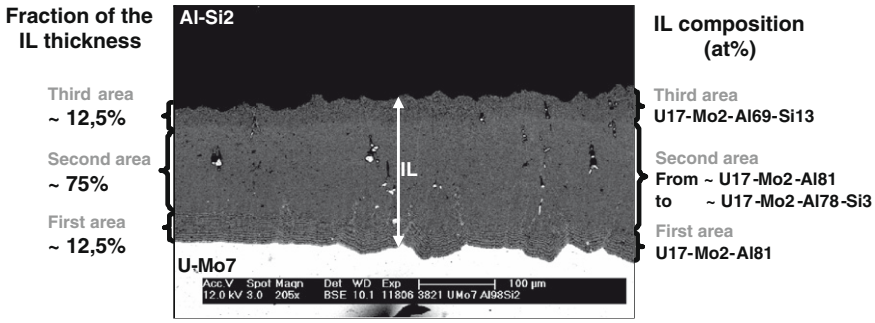

Fig. 2. SEM + EDS typical results obtained on an U–Mo7/Al–Si2 diffusion couple.

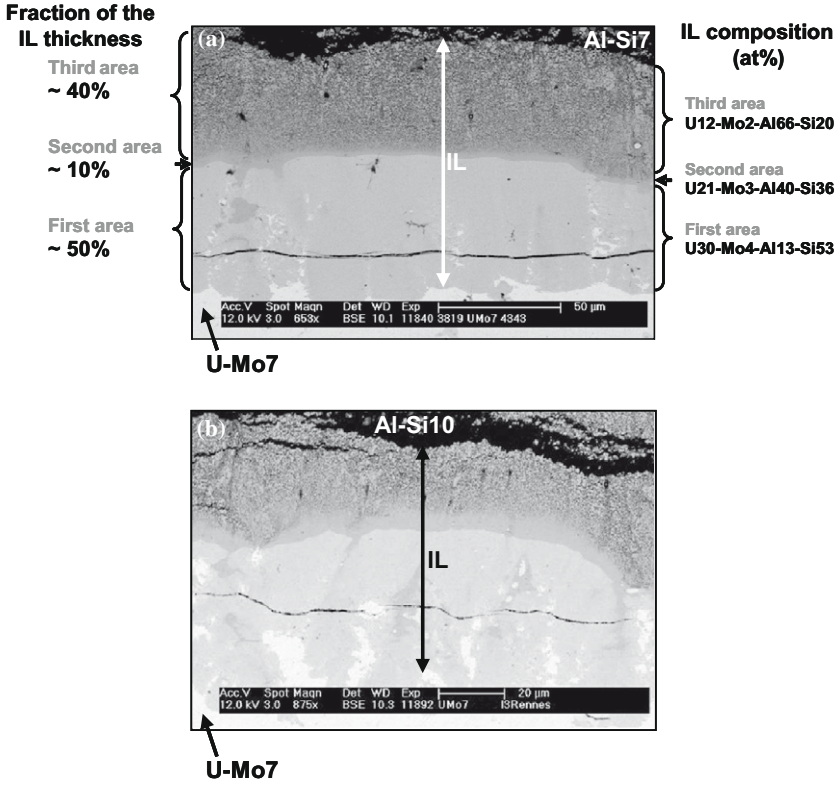

Fig. 3. SEM examinations (BSE mode) on U–Mo7/Al–Si7 and U–Mo10/Al–Si10 diffusion couples. (a) SEM + EDS characterization of the IL, in an U–Mo7/Al–Si7 sample. (b) SEM micrograph of an U–Mo7/Al–Si10 sample.

Contrary to the type 1 IL, type 2 IL is characterized by an evolution of the U and Mo concentrations in the IL, an average higher concentration in Si (above 20 at.%) and finally by the presence of the Si richest part of the IL close to the U–Mo side.

Indeed the Si concentration is about 53 at.% in this area, it decreases in the thin intermediate layer (36 at.%) and is only 20 at.% in the sub-layer located close to the Al–Si alloy.

3.1.3. U–Mo/Al–Si interaction with Si = 5 wt.% (types 1 and 2)

In U–Mo7/Al–Si5 diffusion couple, two kinds of interaction layers are present alternatively at the U–Mo/Al–Si interface, as clearly shown in Fig. 4. EDS measurements enabled to show that the characteristics of the thinnest are similar to type 2, whereas the thickest are closer to type 1. To be more specific, in the thickest IL parts, only the third sub-layer of type 1 ILs (that is close to Al–Si) seems to be present since the measured average Si concentration is about 13 at.%. However, in this diffusion couple, SEM observations do not help in confirming this interpretation since these interactions appear to be less clearly stratified than those previously described.

The occurrence of these two kinds of IL could be linked to the heterogeneous distribution of Si precipitates in the Al, since the alternation step of thin and thick areas is of the same order of magnitude as the Al grain size (compare Figs. 1 and 4).

3.1.4. Influence of the additional thermal treatment (350 °C – 2 months)

The results obtained for diffusion couples annealed at 450 °C are also valid for those further annealed at 350 °C during 2 months. Indeed, no significant evolution of the ILs thicknesses and compositions has been measured.

3.2. μ-XRD characterization of ILs

In this part, the crystallographic composition of ILs types 1 and 2 obtained by μ-XRD measurements on diffusion couples annealed at 450 °C are first presented. Then they are compared to the results obtained on the thin and thick parts of the IL in U–Mo7/Al–Si5. The last section deals with the influence of the second annealing (350 °C – 2 months).

Figs. 5–10 summarize the results obtained on the three diffusion couples of interest: U–Mo7/Al–Si2 (Figs. 5 and 6), U–Mo7/Al–Si7 (Figs. 7 and 8) and U–Mo7/Al–Si5 (Figs. 9 and 10). For a sake of clarity, the presence of impurities such as UO_2 in U–Mo is not reported.

ILs have been found to consist of mainly four phases, two ternary phases (UMo_2Al_{20} and $U_6Mo_4Al_{43}$) and two binary ones ($U(Al, Si)_3$ and $U_3(Si, Al)_5$). Their crystallite size is low compared to the X-ray beam size leading to well defined Debye–Scherrer rings (cf. Figs. 5 and 7). This is not the case for γ-U–Mo and Al phases since only single crystal like diffraction patterns are obtained. For these two last phases, the error associated to their weight fraction determination is thus higher. The obtained weight fractions for UMo_2Al_{20}, $U_6Mo_4Al_{43}$, $U(Al, Si)_3$ and $U_3(Si, Al)_5$ should be considered as semi-quantitative since no correction for absorption and particle size (so-called Brindley factors) has been performed.

Taking into account the beam size, its penetration depth in the sample (especially close to the Al alloy), the sample position and the roughness of the interfaces between sub-layers, transitions between sub-layers are not sharp. To determine the limits (beginning and end) of the three components (Al, U–Mo and IL) of a given diffusion couple or the limits of a sub-layer in the IL (written IL1 and IL2), simple calculations have been performed. For each probed zone of a vertical scan, the weight fractions of the phases making IL1, IL2, IL, U–Mo and Al have been first added and then compared to each others (cf. Figs. 6b and 8b): the component or the sub-layer having the most elevated weight fraction has been reported as the only one in the scheme showing the diffusion couple crystallographic composition (cf. Figs. 6c, 8c and 10). In these last representations (and in the following), normalised weight fractions are indicated for each phase in a given sub-layer.

3.2.1. U–Mo/Al–Si interaction with Si < 5 wt.% (type 1)

In this IL type, the presence of two sub-layers is assessed. In the first, close to the U–Mo side, UAl_3 (80 wt.%) and $U_6Mo_4Al_{43}$ phases (20 wt.%) are present [11,12]. In the second, close to the Al side, the presence of $U(Al, Si)_3$ (88 wt.%) and UMo_2Al_{20} (12 wt.%) phases is evidenced. The Si content of the $U(Al, Si)_3$ phase is estimated to 17 at.% on the basis of its mean cell parameter (about 4.225 Å)

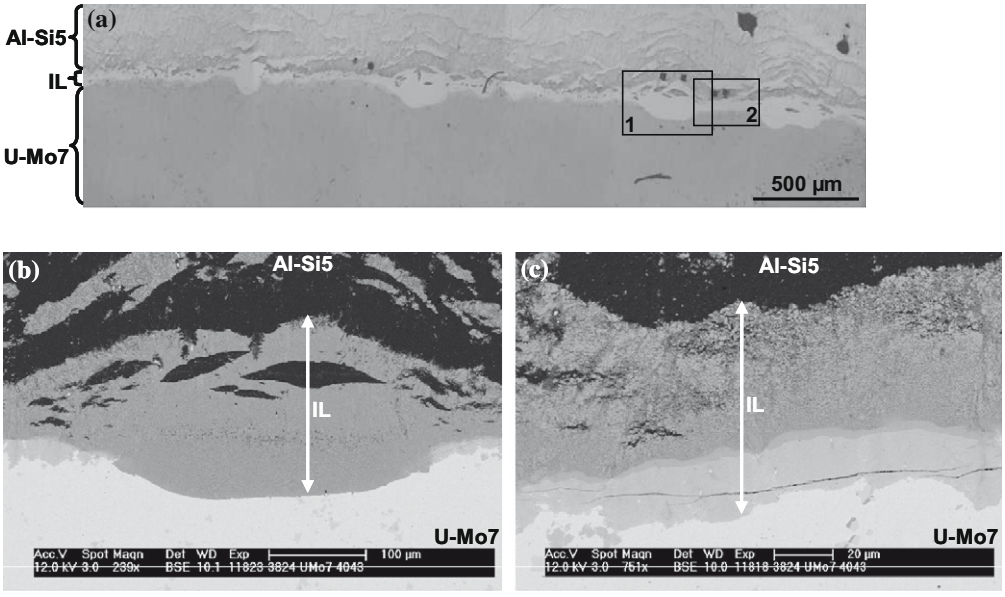

Fig. 4. Examination of the U–Mo7/Al–Si5 diffusion couple. (a) General view (optical microscopy). (b) SEM micrograph (BSE mode) of the zone 1. (c) SEM micrograph (BSE mode) of the zone 2.

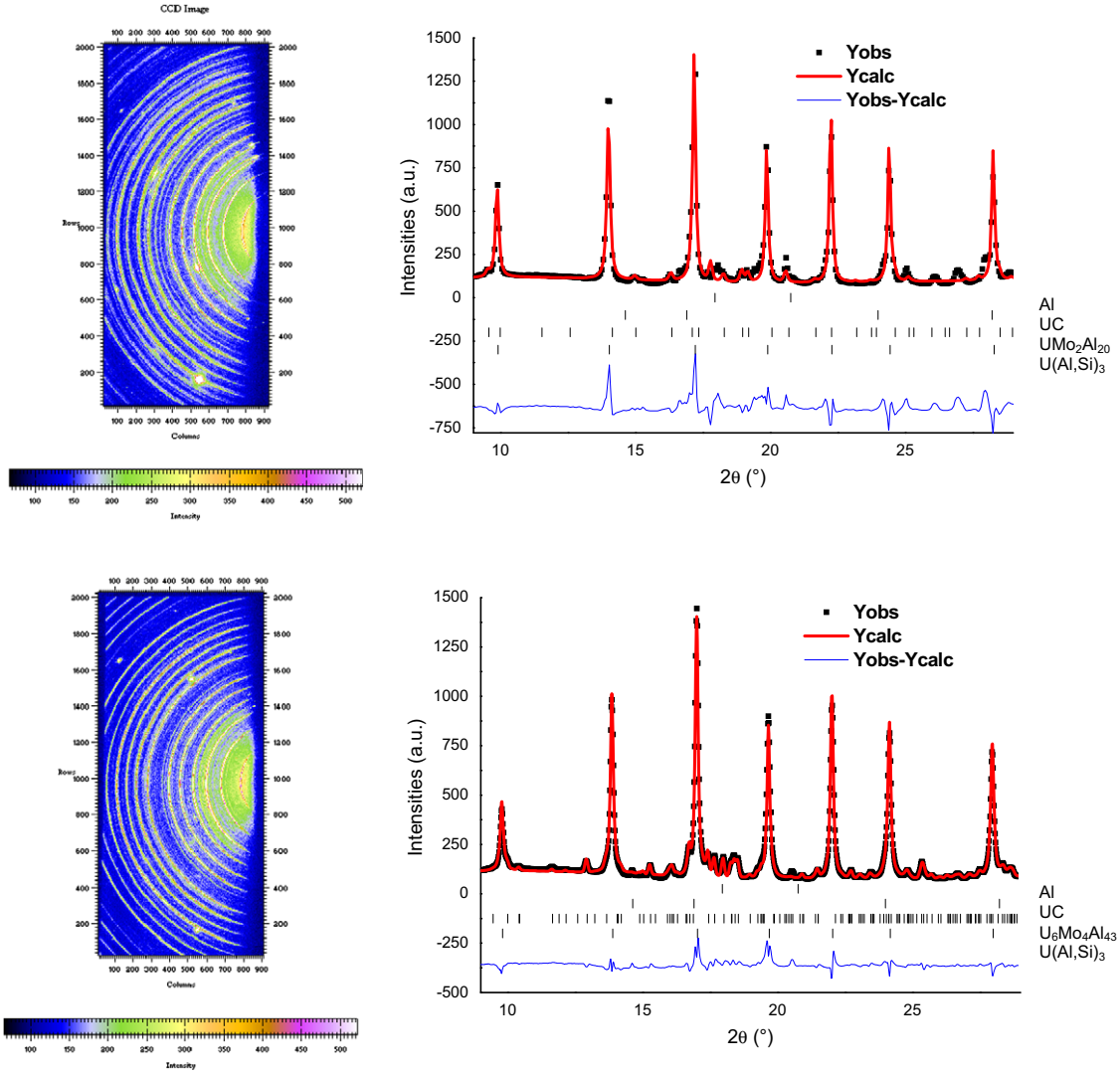

Fig. 5. μ-XRD data collected on the U–Mo7/Al–Si2 diffusion couple and the associated analysis. Images (a) and (b) have been acquired at 100 and 250 μm respectively from the upper part of the vertical scan (see Fig. 6).

and Dwight relation [13]. The composition of both sub-layers seems to be homogeneous in a first approximation. Fluctuations are however mainly due to the presence of Al precipitates.

3.2.2. U–Mo/Al–Si interaction with Si > 5 wt.% (type 2)

Close to the U–Mo side, which was characterized by EDS by its high Si enrichment, an $U_3(Si, Al)_5$ phase (87 wt.%) is found in coexistence with a highly Si enriched $U(Al, Si)_3$ phase (13 wt.%), according to its cell parameter (4.17 Å) [13]. The $U_3(Si, Al)_5$ cell parameters ($a = b = 3.89$ Å and $c = 4.015$ Å) are slightly higher than those of U_3Si_5 pure phase, probably due to some Al substitution.

The thin intermediate layer shown by SEM + EDS examinations is not clearly evidenced by μ-XRD measurements, perhaps because it just corresponds to a transition area, with no specific "signature" in terms of phases. Close to the Al side, as in type 1 ILs, $U(Al, Si)_3$ (84 wt.%) and UMo_2Al_{20} (16 wt.%) phases are present, the Si enrichment of the $U(Al,Si)_3$ phase being greater than that found in type 1 ILs. Indeed the measured $U(Al, Si)_3$ cell parameter is about 4.16 Å in this area.

Note that in the U–Mo area probed by μ-XRD in the characterization reported in Fig. 8, a non-negligible amount of α-U has been detected. Measurements performed at different locations in the U–Mo7/Al–Si7 and U–Mo7/Al–Si10 diffusion couples have demonstrated that the presence of such a phase has not any influence on the IL composition. Considering the limited duration and temperature of the annealing treatment, it is believed that the α-U phase was already present locally in the U–Mo ingot before annealing (even if it was not detected when performing laboratory XRD measurements, due to its low amount).

3.2.3. U–Mo/Al–Si interaction with Si = 5 wt.% (types 1 and 2)

As previously presented, U–Mo7/Al–Si5 couples are characterized by an alternation of thin and thick areas in the IL (cf. Fig. 4). Both types of areas were studied by μ-XRD. The corresponding results, acquired on a sample annealed at 450 °C, are presented in Figs. 9 and 10. The thick parts of the IL (Figs. 9a and 10) are globally mono-layered and composed by two phases: $U(Al, Si)_3$ and UMo_2Al_{20}. Close to U–Mo, the presence of $U_6Mo_4Al_{43}$ and the increase of the $U(Al, Si)_3$ cell parameter from 4.20 Å up to 4.25 Å have also been evidenced, pointing out a decrease in the silicon content in this part of the IL. Note that these phases are the same as those observed in the U–Mo7/Al–Si2 diffusion couple (cf. Fig. 6). On the other hand, the thin parts (Figs. 9b and 10) present two sub-layers:

– a relatively thick one, close to the Al alloy, where $U(Al, Si)_3$ and UMo_2Al_{20} phases are again evidenced,

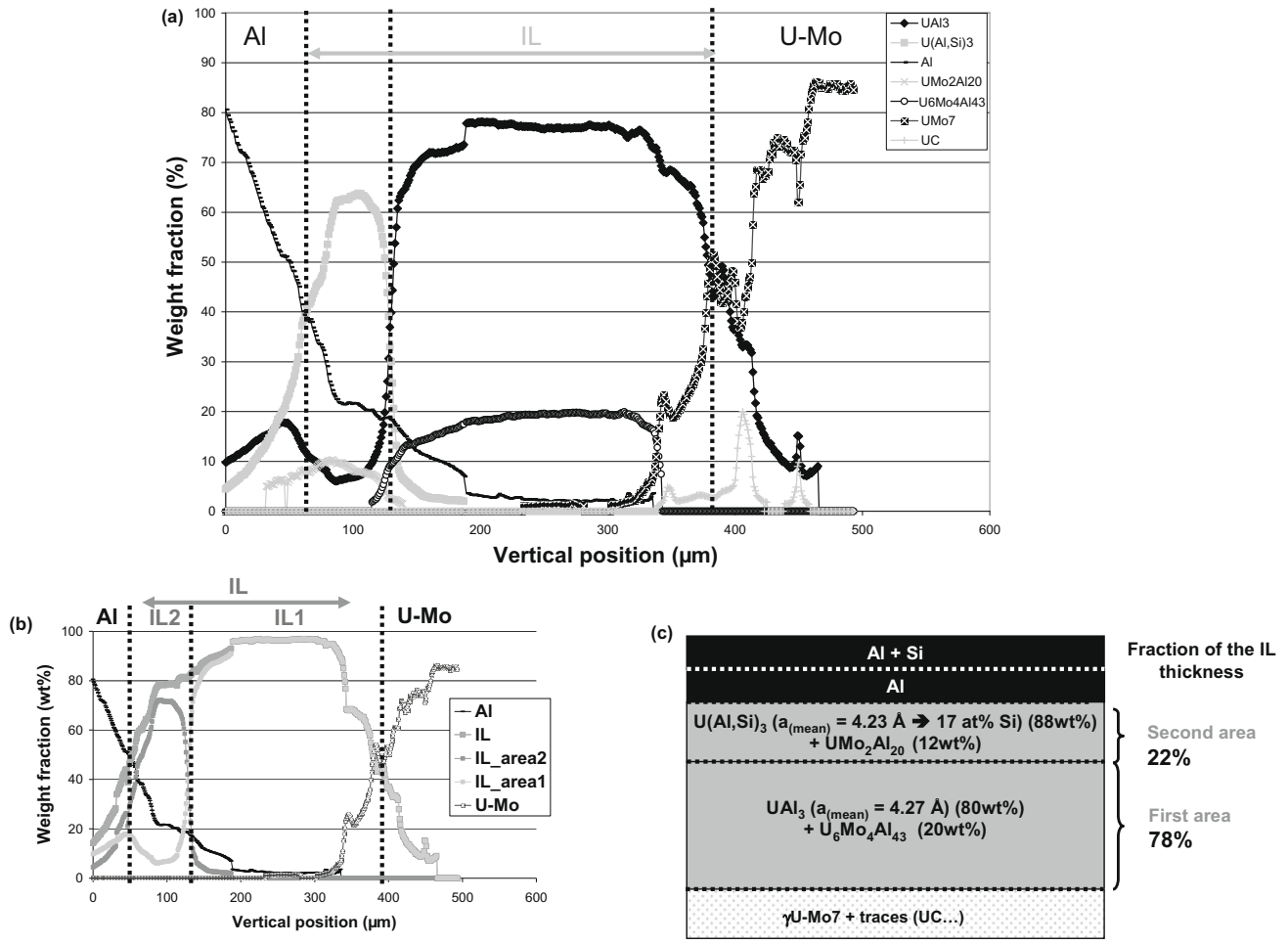

Fig. 6. μ-XRD analysis of an U–Mo7/Al–Si2 diffusion couple. (a) Major phases distribution throughout the IL. (b) Location of the main components of the diffusion couple (Al, IL, U–Mo) and the two sub-layers in the IL. (c) Simplified summary of the results. Semi-quantitative normalised average weight fractions are given in parentheses.

– a thinner one, close to U–Mo, where a significant amount of the $U_3(Si, Al)_5$ phase in found in mixture with the two previous phases,

These results are summarized in Fig. 10. By comparing them with those obtained on types 1 and 2 ILs (cf. Figs. 6b and 8b), it is possible to conclude that:

– the thick parts of the IL correspond to a mono-layered type 1 IL: the second sub-layer, made of $UAl_3 + U_6Mo_4Al_{43}$, is not explicitly present (perhaps only for the reason that it did not form yet),
– the thin parts of the IL correspond to a type 2 IL, for which the second sub-layer, containing the $U_3(Si, Al)_5$ is less developed.

It is worth noting that no destabilisation of γ-U–Mo was evidenced beneath the IL contrary to that observed in U–Mo, by Mirandou et al., beneath locally thicker IL areas, in U–Mo7/Al 6061 diffusion couples annealed at 550 °C [4,14].

3.2.4. Influence of the additional thermal treatment (350°C – 2 months)

By comparing the results obtained on diffusion couples annealed at 450 °C with those concerning couples annealed at 350 °C for 2 months, we have checked that no significant evolution occurred in the crystallographic composition and thickness of the IL. However an increase of the grain size of the phases and a massive destabilisation of the underlying γ-U–Mo7 alloy (as expected, by reference to TTT curves [15]) were noticed.

3.3. Comparison between SEM + EDS and μ-XRD results

It has been shown that the analyses performed by μ-XRD, on the one hand, and SEM + EDS, on the other hand, have evidenced two main types of ILs in the U–Mo7/Al–Si interaction system.

In the two following sections, the agreement between SEM + EDS and μ-XRD results, for each IL types (1 and 2), is analyzed. To enable a discussion on the elementary composition of each sub-layer, Tables 2 and 3 are provided. They compare the results derived from both characterizations for IL types 1 and 2 respectively. Note that μ-XRD results have been obtained by using the normalised average weight fractions of the main phases. They are reported in the schematic representation of each IL type (cf. Figs. 6c and 8c). It is believed that the accuracy of SEM results is higher than that provided by the Rietveld analysis of μ-XRD diagrams, mainly since no Brindley factor has been taken into account (see Section 3.2) and since the Al content of the $U_3(Al, Si)_5$ phase is difficult to determine (it has been assumed that this phase was Al free).

In other words, slight discrepancies found in the elementary composition of a given sub-layer, are to be attributed to the lower accuracy of the μ-XRD analysis detailed in this work.

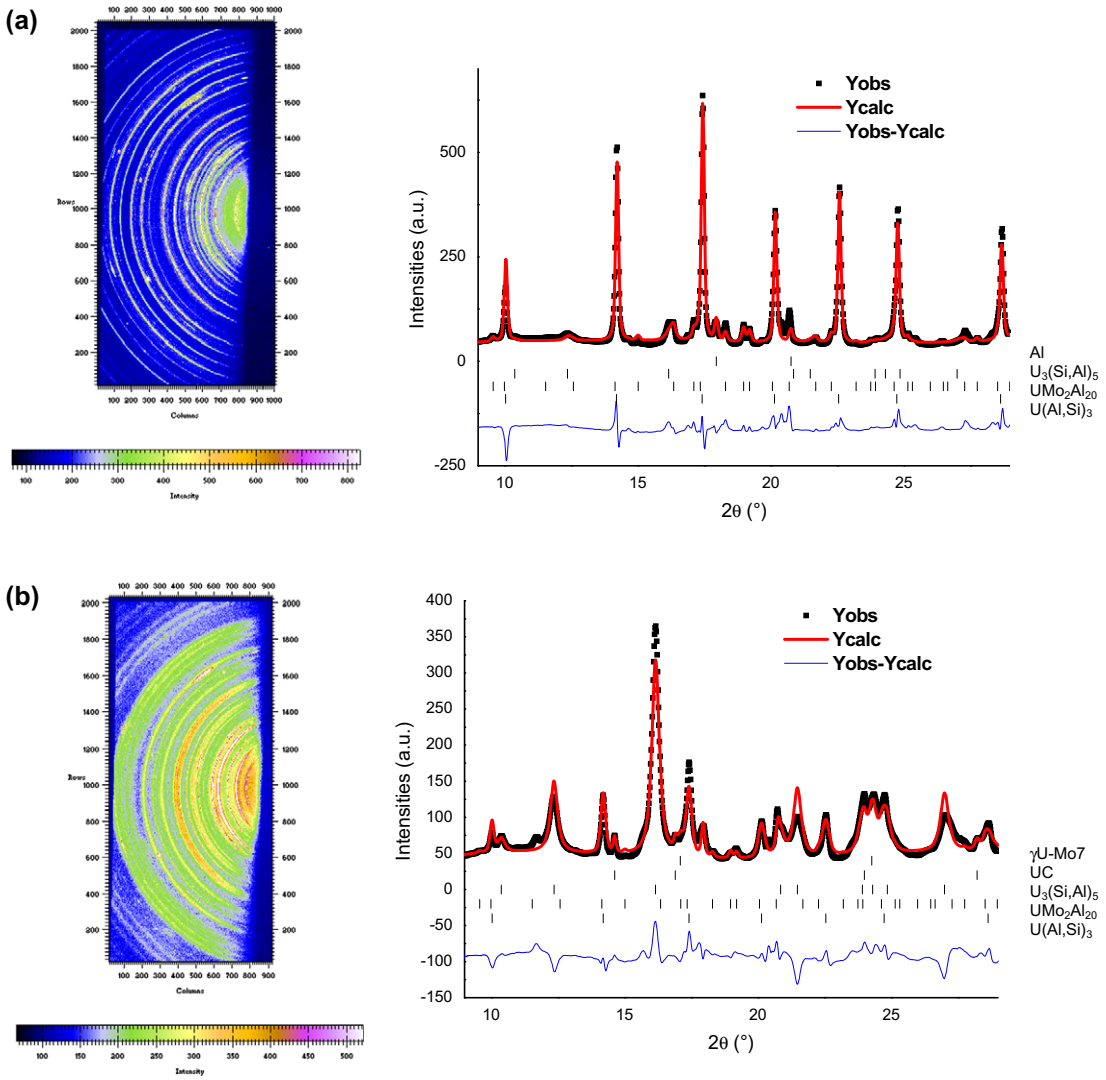

Fig. 7. μ-XRD data collected on the U–Mo7/Al–Si7 diffusion couple and the associated analysis. Images (a) and (b) have been acquired at 80 and 110 μm respectively from the upper part of the vertical scan (see Fig. 8).

3.3.1. U–Mo/Al–Si interaction with Si < 5 wt.% (type 1)

In the type 1 ILs, the conclusions of both analyses are in excellent agreement even if a contradiction seems to exist in the number of sub-layers: three are identified by SEM + EDS when only two are evidenced through the μ-XRD study.

This apparent difference is due to the inability of μ-XRD to distinguish the sub-layer located close to the U–Mo side (area 1 in Fig. 2) from the thickest intermediate one (area 2 in Fig. 2). Indeed their elementary compositions and in particular their silicon concentration only differ by less than 3 at.%. Let's make the hypothesis that this silicon amount will be located in the $U(Al, Si)_3$ phase. The shift in cell parameter induced by this insertion would be very limited (4.251 Å against 4.266 Å) and thus difficult to assess by μ-XRD.

If areas 1 and 2 deduced from the SEM + EDS study are gathered together, the thicknesses and compositions of the two resulting zones are then consistent with those obtained by μ-XRD.

The existence of a silicon poor (or free) sub-layer close to the U–Mo is clearly demonstrated by EDS + SEM and confirmed by the measurement of the cell parameter of UAl_3 phase (4.266 Å).

The second silicon rich (13 at.%) sub-layer close to the Al–Si, identified by SEM, is also evidenced by the decrease of the $U(Al,Si)_3$ cell parameter (cf. Table 2). The relative thicknesses of each sub-layer are 87.5–12.5% (for areas 1 and 2 respectively), as given by SEM + EDS, and 78–22%, as determined by μ-XRD. Taking into account the uncertainties of each type of measurement (especially for μ-XRD) and the local IL irregularities, these results are in good agreement.

Both types of analyses confirm the presence of Mo in each sub-layer of the IL. One can reasonably assume that this element is mainly present in the ternary compounds $U_6Mo_4Al_{43}$ and UMo_2Al_{20}, in the sub-layers which contain these phases, as in the case of U–Mo/Al system [11].

More generally, the elementary compositions of each sub-layer given by both techniques (SEM-EDS and μ-XRD) are in excellent agreement (cf. Table 2).

3.3.2. U–Mo/Al–Si interaction with Si > 5 wt.% (type 2)

As in the previous section, SEM + EDS results are again consistent with the μ-XRD analyses, even if the thin intermediate layer evidenced by SEM + EDS does not appear clearly in μ-XRD results. This sub-layer could therefore correspond to a transition area that would not involve new phases. Moreover, both techniques give very close results for the thickness of each sub-layer: 55–45% for SEM + EDS and 56–44% for μ-XRD. Thicknesses derived from SEM + EDS measurements, have been obtained by dividing into two equal parts the thickness of the intermediate part and

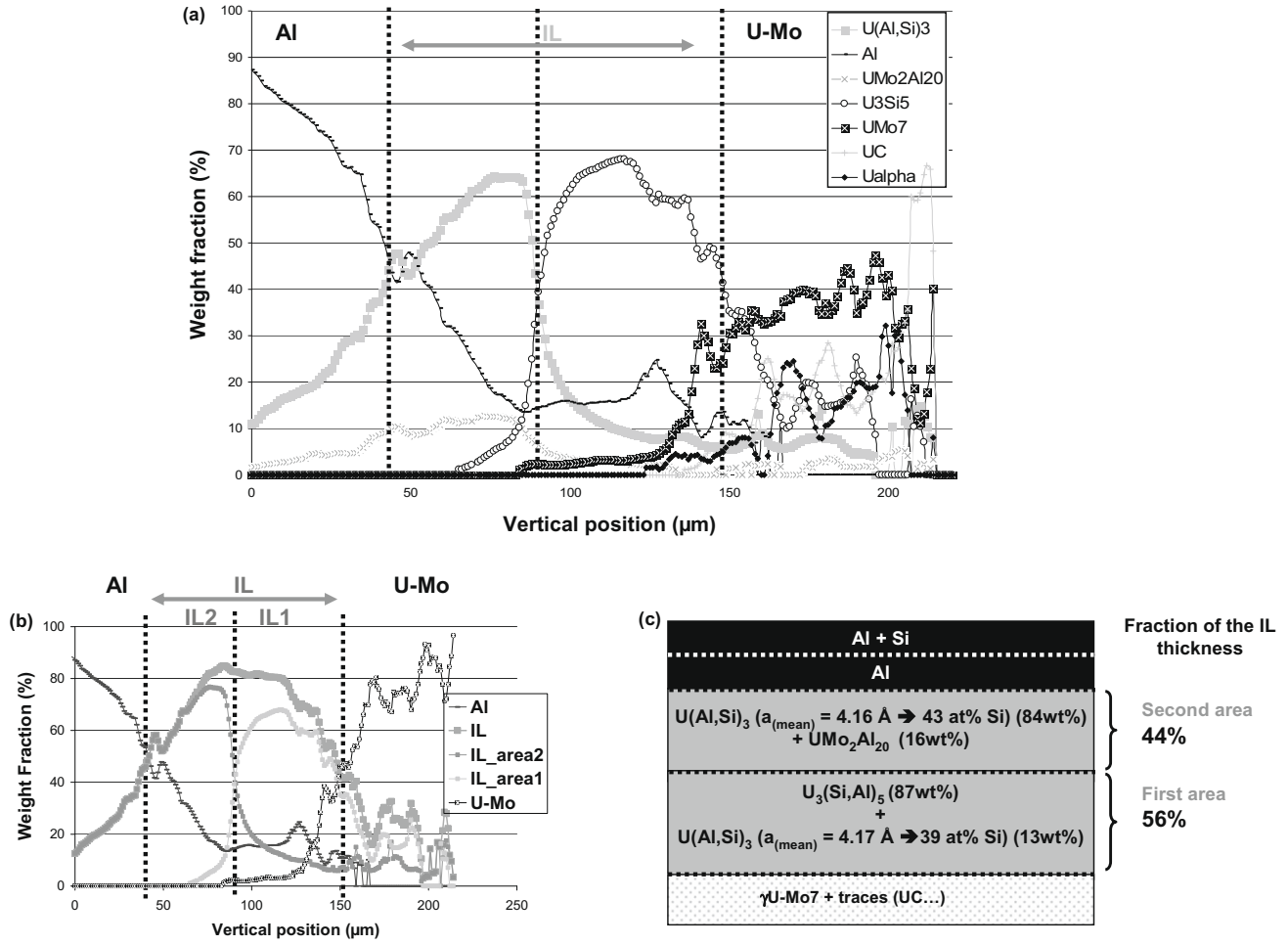

Fig. 8. µ-XRD analysis of an U–Mo7/Al–Si7 diffusion couple. (a) Major phases distribution throughout the IL. (b) Location of the main components of the diffusion couple (Al, IL, U–Mo) and the two sub-layers in the IL. (c) Simplified summary of the results. Semi-quantitative normalised average weight fractions are given in parentheses.

adding them to the two located close to U–Mo and Al–Si respectively.

Finally both techniques show that the Si content into the IL is higher close to the U–Mo7 side than close to the Al–Si alloy (cf. Table 3). More generally semi-quantitative elementary analyses of both sub-layers provided by each technique (SEM–EDS on the one hand and µ-XRD on the other hand) are in very good agreement for Si and Mo when some discrepancies are noted for U and Al (cf. Table 3).

If the behaviour of Mo, in type 1 ILs, can be reasonably predicted, this is not the case for the type 2 ones, especially in the $U_3(Si, Al)_5$ + $U(Al, Si)_3$ sub-layers close to U–Mo. To tackle this issue, characterizations using micro X-ray fluorescence and absorption spectroscopy would be needed.

4. Discussion

This discussion is based on the result obtained in this work and those already reported in literature. It is divided in two parts: the first is devoted to an evaluation of the temperature influence on the composition of the U–Mo/Al–Si interaction layer and the second to a mechanistic description of the U–Mo/Al–Si interactions.

4.1. Influence of temperature

In this work, U–Mo/Al–Si ILs have been studied at 450 °C. For determining the additional influence of temperature on the nature of U–Mo/Al–Si IL, the study of data already reported in the literature was required.

4.1.1. Type 1 IL

Type 1-like layers have been characterized by Park et al., using EPMA, in two different diffusion couples annealed at higher temperatures (respectively 580 and 600 °C) [7], demonstrating the occurrence of this IL type in this temperature range.

In the first diffusion couple, U–Mo7/Al–Si2 annealed at 580 °C for 5 h, the measured Si concentration profiles appear to be indeed similar to those collected on our type 1 layers, with close (Al + Si)/(U + Mo) ratios, despite differences in the experimental procedures concerning diffusion couples preparation. The second shows that when temperature increases, the U–Mo/Al–Si interaction system tends to evolve to a type 1 one, even if the Si content in Al is relatively high ($\geqslant$5 wt.%). Indeed, these authors have found that in an U–Mo7/Al–Si5 diffusion couple annealed at 600 °C for 3 h, the Si concentration profile in the IL was not far from that of a type 1 IL (the more Si enriched part of the IL being located close to Al), with an (Al + Si)/(U + Mo) ratio of the order of 4 [7]. This suggests that, due to kinetic effects, the reaction of Al with U–Mo is more favoured than that of Si with U–Mo, when the temperature increases.

4.1.2. Type 2 IL

The type 2 U–Mo/Al–Si interaction layer also grows at temperatures above 450 °C (temperature tested in this work) as shown by

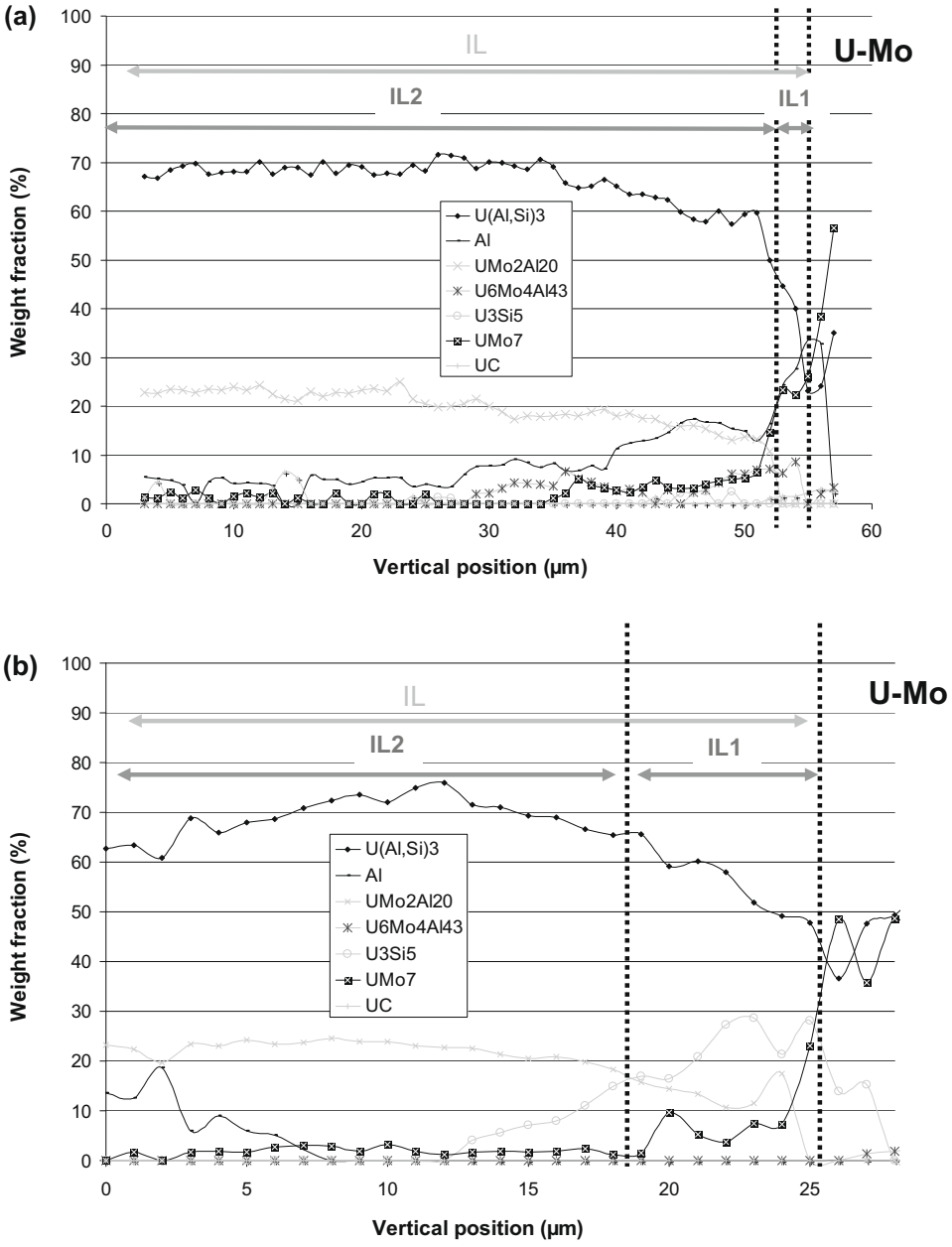

Fig. 9. µ-XRD analysis of an U–Mo7/Al–Si5 diffusion couple. (a) Major phases distribution throughout the IL, in a thick area (cf. Fig. 4). (b) Major phases distribution throughout the IL, in a thin area (cf. Fig. 4).

Mirandou et al. [2–4] on U–Mo7/Al–Si7 diffusion couple annealed at 550 °C.

Thanks to X-ray diffraction using synchrotron radiations, the authors have shown that the IL developed in this sample was made of the following phases: $U(Al, Si)_3 + UMo_2Al_{20} + U_3Si_5$ phases. The results they obtained at 550 °C are fully consistent with our results for type 2 ILs (for a Si content in Al greater than 5 wt.%), in terms of composition and structure of the ILs.

It is not demonstrated that type 2 ILs can form at temperatures below 450 °C. For example at 340 °C, on thinner ILs (about 5–10 µm thick), only $U_3Si_5 + U(Al, Si)_3$ phases were found in a U–Mo7/Al–Si7 diffusion couple [4]. However to be fully considered as a type 2 IL, this IL should have been made of two sub-layers (which does not seem to be the case) and the UMo_2Al_{20} phase should have been found in the IL. Depending on whether one considers that the thickness of this IL has prevented from an accurate characterization or not, this IL is a type 2 or another type of IL.

4.1.3. Conclusion

This literature survey clearly indicates that the two types of IL identified in this work (at 450 °C) also exist at higher temperatures (up to 600 °C). Moreover it points out that the threshold value of 5 wt.% determined in our testing conditions can vary with temperature.

4.2. General mechanistic description of U–Mo/Al–Si interaction process

The main goal of this section is to propose the main mechanisms leading to each of the three U–Mo/Al–Si interactions kinds.

4.2.1. Growth of the first sub-layer in the ILs

Assuming that the reaction product growth occurs at the U–Mo/reaction layer interface, as proposed by Mazaudier et al. [12] on the U–Mo/Al interaction, the oldest part (that appeared firstly) of the ILs is located close to the Al side of the couple. In both types of

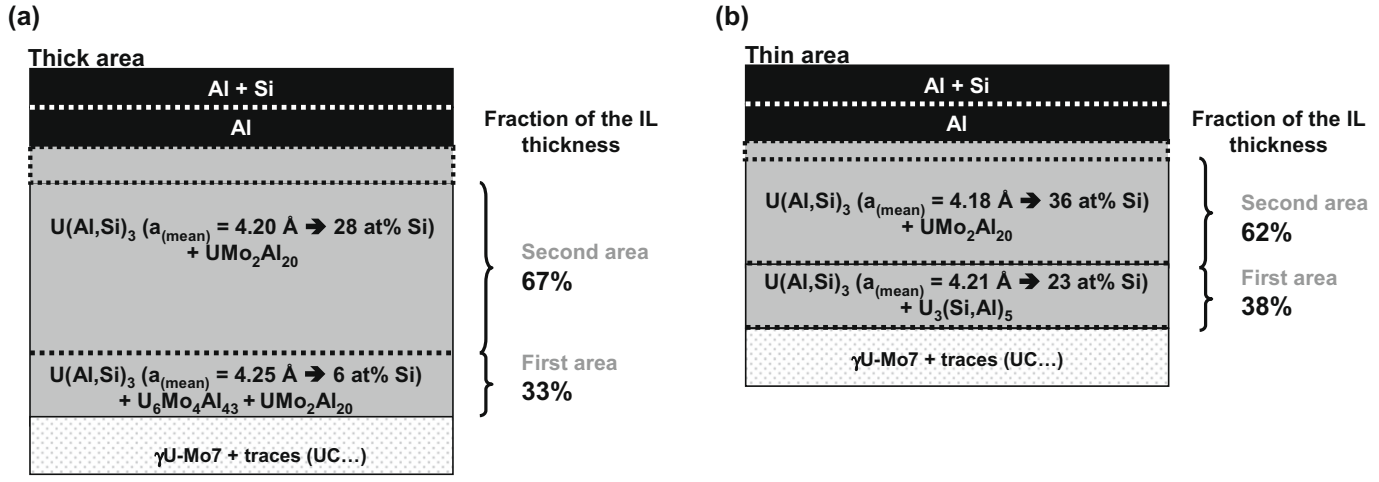

Fig. 10. Result of the μ-XRD study of an U–Mo7/Al–Si5 diffusion couple. (a) Simplified summary of the results for a thick IL (cf. Fig. 4). (b) Simplified summary of the results for a thin IL (cf. Fig. 4).

Table 2
Elementary composition of the two sub-layers of IL type 1 as determined by μ-XRD and EDS on the U–Mo7/Al–Si2 diffusion couple.

	Composition of IL type 1							
	Sub-layer close to Al–Si (IL2)				Sub-layer close to U–Mo7(IL1)			
	U	Mo	Al	Si	U	Mo	Al	Si
SEM	17	2	69	13	17	2	81	0
μ-DRX	21	2	67	10	21	2	77	0

Table 3
Elementary composition of the two sub-layers of IL type 2 as determined by μ-XRD and EDS on the U–Mo7/Al–Si7 diffusion couple.

	Composition of IL type 2							
	Sub-layer close to Al–Si (IL2)				Sub-layer close to U–Mo7(IL1)			
	U	Mo	Al	Si	U	Mo	Al	Si
SEM	12	2	66	20	30	4	13	53
μ-DRX	20	2	54	24	35	0	7	52

ILs, it is composed of $U(Al, Si)_3 + UMo_2Al_{20}$ (with a fluctuating Si enrichment of the $U(Al, Si)_3$ phase). This tends to show that, at the beginning of the interaction, in all the studied cases, enough Si is present close to the reactional interface to govern the $U(Al, Si)_3 + UMo_2Al_{20}$ phases formation, instead of $UAl_4 + UMo_2Al_{20}$ when the matrix is made of pure Al [11,12]. This result confirms that Si acts as an inhibitor of the UAl_4 formation, as shown first by Thurber et al. [16] and confirmed later by many other authors.

4.2.2. Growth of the second sub-layer in the ILs

At this stage of the interaction process, Al and Si have to diffuse through this $U(Al, Si)_3 + UMo_2Al_{20}$ layer in order to react with U–Mo. According to Savchenko et al. [17], Si diffuses through $U(Al, Si)_3$ phase much faster than Al. Then, two cases have to be considered:

- *Case 1*: Si depletion in Al, in front of the IL, becomes too important to maintain a sufficient silicon diffusion flux, through the IL, and the interaction system becomes dominated by Al diffusion (i.e. identical to that observed in U–Mo/Al diffusion couples).
- *Case 2*: despite of a progressive Si depletion in Al, a sufficient Si diffusion flux through the IL can be kept (at least during a certain time), leading to the formation of an U_3Si_5 silicide phase, close to the U–Mo side.

On this basis, the case 1 should logically lead to a type 1 IL and the case 2, to a type 2 one, as illustrated by the two first schemes presented in Fig. 11. Complementary experiments including the characterization of couples obtained after different annealing durations could give interesting clues regarding these hypotheses.

Another point to note is the detection of Al in the ILs, far from the Al/IL interface (cf. Figs. 6 and 8). Close to this interface, different effects could explain the detection of Al in the IL: roughness effects, position of the X-ray beam by reference to it (not perfectly parallel), absorption effects of X-rays, etc. Far from this interface, as proposed by Savchenko, this Al could be rejected by the UX_3 phase, in the framework of a substitution process of Al by Si [17]. The SEM + EDS examinations performed in this work did not reveal any Al precipitates in the IL, probably because they are nanometre sized. TEM examinations could be useful for checking this point.

4.2.3. Important parameters driving the growth of types 1 and 2 ILs

In addition to Si content in the Al–Si alloy, first importance parameters are of course temperature and time because they influence directly the activation of diffusion processes and especially the diffusion kinetics of Al and Si in Al and in the IL (more especially in the UX_3 phase). To our knowledge, data concerning these kinetics are lacking. It would be very interesting to obtain such

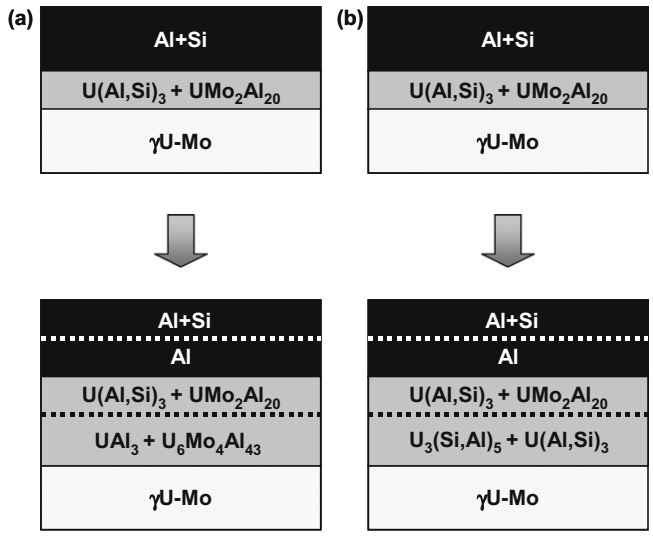

Fig. 11. Kinetic evolutions of the composition of 2 kinds of IL identified in the U–Mo/Al–Si interaction system. Schematic representations for type 1 (a) and type 2 (b).

data and to use them for modelling the thermally activated U–Mo/Al–Si interaction process.

Keeping in mind that in U–Mo7/Al–Si5 couples ("threshold couples" in this study), variations of the IL thickness seem to be linked to the Al grain size, it is likely that the local distribution of Si plays also a major role in these phenomena. Studying couples obtained with Al–Si alloys which are characterized by significantly different Si precipitates distributions (if it is possible to maintain significant differences at the annealing temperature) could also give additional information about the mechanisms to be considered.

4.3. Conclusions

The occurrence of at least two types of ILs in U–Mo/Al–Si diffusion couples seems to be directly linked to (i) the Si content and distribution in the Al alloy (thin or coarse precipitates, more or less numerous), (ii) the diffusion conditions (temperature and time), (iii) the reacting interface characteristics. Concerning this last point, differences between the way of preparing surfaces and clamping them during their annealing can certainly influence the interaction process, in U–Mo/Al–Si diffusion couples. Such differences are obvious when speaking about fuel plates with U–Mo particles dispersed in an Al–Si matrix, compared with diffusion couples. These are probably the reasons why the formation of one type of IL or the other cannot be simply associated to a Si threshold value and/or specific annealing conditions. Some differences between the results obtained in this study and those of other authors (see for example [2–4,7,18–20]) could be explained on this basis.

5. Conclusions

Using a set of U–Mo7/Al–Si diffusion couples, with silicon content ranging from 2 wt.% to 10 wt.%, U–Mo/Al–Si interactions were obtained by thermal annealing. The elementary composition, the microstructure and the structural properties of these couples, were systematically characterized by SEM + EDS and by μ-XRD. Thanks to these characterizations, two main types of interaction layers (ILs) were evidenced, depending on the silicon content in the aluminium alloy, with a threshold value of about 5 wt.% (in the conditions tested in this study). Below this threshold value, the ILs are mainly bi-layered: a first sub-layer, close to U–Mo, containing the $UAl_3 + U_6Mo_4Al_{43}$ phases and a second one, close to Al–Si, with the $U(Al, Si)_3 + UMo_2Al_{20}$ phases. Above this threshold, the ILs are again mainly bi-layered, with an $U_3(Si, Al)_5 + U(Al, Si)_3$ sub-layer, close to U–Mo, and an $U(Al, Si)_3 + UMo_2Al_{20}$ sub-layer, close to Al–Si.

According to literature data, it can be not excluded that a third type of IL exists, when the interaction occurs at a relatively low temperature. In this case it would consist of $U_3(Si, Al)_5 + U(Al, Si)_3$ phases (the $U_3(Si, Al)_5$ being predominant). Further experimental work would be however needed to state definitely on that point.

The occurrence of the different types of ILs in U–Mo/Al–Si diffusion couples seem to be directly linked to (i) the Si content and distribution in the Al alloy, (ii) the diffusion conditions, (iii) the reacting interface characteristics. For these reasons, the formation of one type of IL or the other cannot be simply associated to threshold values for Si content and temperature.

Finally, the conclusions of this study should be also interesting from a technological point of view, since one current promising solution for optimizing these fuel performances is to use this U–Mo/Al–Si interactions for growing a Si rich protective layer around the U–Mo particles during the fuel plate manufacturing step (see Section 1). Indeed it clearly states that the choice of the thermal treatment temperature as well as the Si weight fraction will not only have an influence on the thickness of this coating but also on its microstructure and its crystallographic composition. No comparative data on the in-pile efficiency of coatings based on $U(Al, Si)_3$ or U_3Si_5 are currently available in literature: this point has to be investigated.

Acknowledgments

C. Jarousse and M. Grasse, from AREVA-CERCA (Romans, France) are gratefully acknowledged for supplying the U–Mo samples used in this study. J. Miragaya and L. Silvestre (CEA/Cadarache) are warmly thanked for diffusion couples preparation.

References

[1] A. Leenaers, S. Van den Berghe, E. Koonen, C. Jarousse, F. Huet, M. Trotabas, M. Boyard, S. Guillot, L. Sannen, M. Verwerft, J. Nucl. Mater. 335 (2004) 39.
[2] M. Mirandou, S. Arico, S. Balart, L. Gribaudo, A.M. Fortis, in: Proceedings of the 2007 RERTR International Meeting, Prague, Czech Republic, September 23–27, 2007.
[3] M. Mirandou, S. Arico, M. Rosenbusch, M. Ortiz, S. Balart, L. Gribaudo, J. Nucl. Mater. 384 (2009) 268.
[4] M. Mirandou, S.F. Arico, S.N. Balart, L.M. Gribaudo, Mater. Charact. 60 (2009) 888.
[5] M. Cornen, M. Rodier, X. Iltis, S. Dubois, P. Lemoine, in: Proceedings of the 2008 RRFM ENS Meeting, Hamburg, Germany, March 2–5, 2008.
[6] M. Cornen, X. Iltis, F. Mazaudier, S. Dubois, P. Lemoine, in: Proceedings of the 2007 MRS Fall Meeting, Boston, USA, November 27–29, 2007.
[7] J.M. Park, H.J. Ryu, S.J. Oh, D.B. Lee, C.K. Kim, Y.S. Kim, G.L. Hofman, J. Nucl. Mater. 374 (2008) 422.
[8] D.D. Keiser, A.B. Robinson, D.E. Janney, J.F. Jue, in: Proceedings of the 2008 RRFM ENS Meeting, Hamburg, Germany, March 2–5, 2008.
[9] A. Leenaers, S. Van den Berghe, S. Dubois, J. Noirot, M. Ripert, P. Lemoine, in: Proceedings of the 2008 RRFM ENS Meeting, Hamburg, Germany, March 2–5, 2008.
[10] A. Leenaers, C. Detavernier, S. Van den Berghe, J. Nucl. Mater. 381 (2008) 242.
[11] H. Palancher, Ph. Martin, V. Nassif, R. Tucoulou, O. Proux, J.L. Hazemann, O. Tougait, E. Lahéra, F. Mazaudier, C. Valot, S. Dubois, J. Appl. Crystallogr. 40 (2007) 1064.
[12] F. Mazaudier, C. Proye, F. Hodaj, J. Nucl. Mater. 377 (2008) 476.
[13] A.E. Dwight, ANL 82-14 Report, September 1982.
[14] C. Komar Varela, M. Mirandou, S. Arico, S. Balart, L. Gribaudo, in: Proceedings of the 2007 RRFM ENS Meeting, Lyon, France, March 11–15, 2007.
[15] P.E. Repas, R.H. Goodenow, R.F. Hehemann, Trans. ASM 57 (1964) 150.
[16] W.C. Thurber, R.J. Beaver, ORNL-2602 Report, 1959.
[17] A. Savchenko, A. Vatulin, I. Dobrikova, Y. Konovalov, in: Proceedings of the 2006 RRFM ENS Meeting, Sofia, Bulgaria, 30 April–3 May, 2006.
[18] H.J. Ryu, J.M. Park, C.K. Kim, Y.S. Kim, G.L. Hofman, J. Phase Equilibr. Diffus. 27 (2006) 651.
[19] H.J. Ryu, J.M. Park, C.K. Kim, Y.S. Kim, in: Proceedings of the 2008 RERTR International Meeting, Washington DC, USA, October 5–9, 2008.
[20] L. Olivares, J. Marin, M. Barrera, G. Torres, J. Lisboa, in: Proceedings of the 2007 RERTR International Meeting, Prague, Czech Republic, September 23–27, 2007.